Supporting Information

Vecchiarelli et al. 10.1073/pnas.1401025111

SI Text

Calculation of the Bead Trajectory Mean Square Displacement and Fitting the Mean Square Displacement to Obtain the Diffusion Constant and Bias Force. Mean square displacement (MSD) as a function of time interval was calculated for each trajectory as follows (1, 2):

$$MSD(\Delta t) \equiv MSD(j) = \frac{1}{(n-j)} \sum_{i-0}^{n-j} [r(i+j) - r(i)]^2, \mathrm{j} < \mathrm{n}; \Delta t = j\tau,$$

where n is the total number of video frames, τ is the video frame period, and frames are indexed over i. The position r was calculated from the x, and y coordinates of the position of the bead in each frame:

$$r = \sqrt{x^2 + y^2}.$$

To quantify the diffusion and biased motion of the beads, the MSD curves were fit with the following expression:

$$MSD = a_0 + a_1 t + a_2 t^2.$$

For pure diffusion in two dimensions, $a_0 = 2\sigma^2$, where σ is the position tracking uncertainty, $a_1 = 4D$, where D is the diffusion constant, and $a_2 = 0$.

If the particle additionally undergoes directional biased motion with velocity v, then $a_2 = v^2$. Therefore, both the diffusion constant, D, and the particle velocity, v, could be obtained by fitting the MSD curve with the above expression.

Under the assumption that the velocity of the directed beads is determined by a balance between the applied force, F, and the drag on the bead, β: $v = F/\beta$, the force can be estimated via the Einstein–Smoluchowski relation:

$$D = \frac{k_B T}{\beta},$$

where $k_B T$ is the thermal energy. Combining expressions leads to the following expression for the force on the bead in terms of the measured quantities:

$$F = v \frac{k_B T}{D}.$$

The average force on the directed beads calculated from this analysis is 12 ± 4 fN (10^{-15} N) (uncertainty is SEM).

Calculation of Vertical and Pairwise Repulsive Forces on Dynal MyOne Beads. The magnetization per kilogram of the MyOne Dynabeads (Invitrogen) in an external field is described by a Langevin function:

$$\vec{m}(B) = \vec{m}[\coth(B/B_0) - B/B_0].$$

The manufacturer provided numbers are $m_{sat} = 22\ \mathrm{J{\cdot}T^{-1}{\cdot}kg^{-1}}$, $B_0 = 18{\cdot}10^{-3}$ T, and B is the external field in tesla. The density of the MyOne beads is 1.8 g/cm^3 and their radius is 1.05 μm, resulting in a mass per bead of $1.1{\cdot}10^{-15}$ kg. The induced magnetic moment of the bead will interact with the applied field resulting in potential energy:

$$U = \vec{m}(B) \cdot \vec{B},$$

and the force on the bead:

$$F = -\vec{m}(B) \cdot \nabla \vec{B}.$$

The field directly below the magnet [N 52, cylindrical magnet 1.5" (38.1 mm) in length and 1/4" (6.35 mm) in diameter; K&J Magnetics] as a function of the separation from the end of the long axis of the magnet was estimated with software on the K&J Magnetics Web site (www.kjmagnetics.com/). At ∼12-mm separation between the magnet and the top of the imaging chamber, the field is ∼0.025 T and the gradient is $\sim 4\ \mathrm{T{\cdot}M^{-1}}$. The magnetization at this field strength is $\sim 1{\cdot}10^{-14}\ \mathrm{J{\cdot}T^{-1}}$ and the upward force on the bead is ∼0.04 pN (10^{-12} N), which is approximately fourfold larger than the force of gravity on the bead, neglecting the buoyant force of 0.006 pN. Upward force on Dynal MyOne magnetic bead as a function of the distance between the end of the magnet and the surface of the flow cell (Fig. S5*A*).

The field of the cylindrical magnet at the surface of the flow cell points in the vertical direction. The magnetic beads will therefore be magnetized along this direction, and as a result they repel each other. The repulsive force in a plane perpendicular to the dipole orientation between two equally magnetized spheres with aligned dipoles is as follows (3):

$$F = \frac{3\mu_0 M^2}{4\pi r^4}.$$

Here, M is the magnetization of the sphere in joules per tesla, and r is the separation between the centers of the spheres in meters. Assuming $M \sim 1{\cdot}10^{-14}\ \mathrm{J{\cdot}T^{-1}}$, and $r \sim 9$ μm gives a deflection force of ∼0.005 pN, with a range of ∼0.007 pN at 8 μm and ∼0.003 pN at 10 μm. The equation provides a measure of the repulsive force on the beads (assuming ∼12 mm magnet separation and $M \sim 1{\cdot}10^{-14}\ \mathrm{J{\cdot}T^{-1}}$) as a function of the center-to-center distance (Fig. S5*B*).

Estimate of the Chemophoresis Force on a SopB-Bound Bead Interacting with a SopA Surface Gradient. The reaction diffusion process of the Sop system generates a SopA concentration gradient on the DNA carpet that can produce a force that biases the motion of the SopB-coated beads (Fig. S6). Under the nonequilibrium conditions of a SopA concentration gradient, the total energy of the combined system will decrease as an increasing number of molecules of SopB bind SopA. Because SopA and SopB concentrations are nonuniform, this spatially dependent binding energy results in a directional force on the SopB-coated bead, proportional to, and in the direction of, the SopA gradient. The resulting force depends on the reactant concentrations, the gradient of the SopA concentration, and the effective K_d of the SopA–SopB interaction.

Sugawara and Kaneko (4) have derived an expression for this force, which they termed the "chemophoresis" force. Rewriting equation 3 from ref. 4, we arrive at the following expression for the force:

$$F = n \frac{\chi(r)}{K_d + \chi(r)} \nabla \mu(r),$$

where F is the force on the bead, n is the number of SopB molecules on the bead that can interact with the surface-bound SopA, $\chi(r)$ is the spatially varying SopA concentration, K_d is the effective SopB–SopA disassociation constant in the context of

the local environment of the reaction, and $\mu(r)$ is the chemical potential associated with the spatially varying SopA concentration. The chemical potential μ is related to the concentration of SopA: $\mu(r) = \mu_0 + k_BT\cdot\ln[\chi(r)]$, where μ_0 is the standard chemical potential and k_BT is the thermal energy. To estimate the force on the SopB-coated bead, we must estimate (*i*) the number, *n,* of SopB molecules on the bead that can bind carpet-bound SopA, (*ii*) the spatial concentration of SopA on the surface, and (*iii*) the disassociation constant K_d. For this estimate of the force, we treat the experimentally observed SopA gradient in the vicinity of the translocating SopB-coated bead as constant by obtaining the average parameters from 12 typical examples. The full dynamic calculation in which the motion of the bead and the resulting change in the SopA concentration profile are dynamically established is significantly more involved. The additional details of the reaction diffusion mechanism that establishes the SopA concentration gradient requires many kinetic parameters that are currently unavailable.

The number *n* of bound SopB molecules that can interact with surface-bound SopA can be roughly estimated from the properties of the DNA fragments containing *sopC* binding sites that are attached to the magnetic bead. Twelve repeats of the 43-bp *sopC* binding sequence (516 bp) are located in the middle of a 3-kb DNA fragment, one end of which is attached to the bead via a biotin-streptavidin linkage. Assuming a 50-nm persistence length (p), the distance between the end of the DNA and the *sopC* sites (R_{rms}) is as follows:

$$R_{rms} \approx \sqrt{2Lp} \approx 225 \text{ nm}.$$

We estimate that there are ~1,000 ± 200 DNA molecules per bead (see above). Because the magnetic moment of the bead is aligned with the external vertical magnetic field, the beads cannot "roll" on the surface. Therefore, we assume only *sopC* sites within R_{rms} of the surface contribute "active" binding sites, which corresponds to a fraction, $R_{rms}/(2\cdot R_{bead}) \sim 0.2$, of the total DNA on the bead. We assume that each DNA molecule is bound by ~12 SopB dimers so the total number of SopB molecules that can bind SopA is on the order of 4,800. This value is likely an overestimate by severalfold and difficult to compute accurately, considering that SopB molecules bound to *sopC*-DNA on the beads can form intra-DNA interactions with SopA on the bead, instead of SopA on the carpet.

We can estimate the surface concentration of SopA from analysis of the fluorescence intensity in the total internal reflection fluorescence (TIRF) movies. In the vicinity of the SopB/*sopC*-coated bead, we estimate that the number of SopA molecules per square micrometer increases by ~4 per pixel (185 nm) along the gradient from the center of a typical depletion zone, which has ~400 SopA molecules per square micrometer. To convert these surface concentrations to a volume concentration gradient, we estimate that the SopA molecules are bound to a layer of DNA carpet on the order of 100-nm thick. Under these assumptions:

$$\chi(x) = 6.6\,\mu\text{M} + 3.6\ 10^{-4}(x)\ \mu\text{M/nm}$$

$$\text{and}\ \ \mu(x) = \mu_0 + k_BT\ln\left(6.6\ \mu\text{M} + 3.6\ 10^{-4}(x)\ \mu\text{M/nm}\right),$$

we can now estimate the force:

$$F(x) = n\frac{k_DT\dfrac{d\chi}{dx}}{K_d + \chi(x)}.$$

For a bead with $n \sim 4{,}800$ interacting SopB molecules sitting about midway on the SopA gradient at $x \sim 3{,}000$ nm, expressing k_BT in units of piconewtons·nanometer and K_d in units of micromolar, the force in piconewtons is as follows:

$$F \approx \frac{7}{K_d + 7.6}.$$

The K_d of the SopA–SopB interaction has not been published to our knowledge under any conditions, and it is difficult to estimate under the conditions relevant to the local environment of this reaction. The forces estimated from the biased motion are on the order of 12 fN (see above) corresponding to an effective K_d on the order of 570 μM. If competition by the bead-bound SopA for SopB, and other overestimation errors, reduces the effective number of SopB available to interact with carpet-bound SopA by an order of magnitude, an effective K_d of 51 μM would result in 12 fN of driving force. Given the relatively large uncertainties in estimating the relevant geometrical parameters and the reactant concentrations, and the uncertainties in the experimentally obtained estimates of the force, we consider the K_d value needed to produce the estimated driving force reasonable. For a more realistic quantitative consideration, a substantially refined model simulation with expanded parameters would be needed. Nevertheless, with the above exercise, we conclude that the "chemophoresis" model, as part of our diffusion-ratchet mechanism, could easily explain the observed bead motion in our experiments.

1. Qian H, Sheetz MP, Elson EL (1991) Single particle tracking. Analysis of diffusion and flow in two-dimensional systems. *Biophys J* 60(4):910–921.
2. Sarkar SK, Marmer B, Goldberg G, Neuman KC (2012) Single-molecule tracking of collagenase on native type I collagen fibrils reveals degradation mechanism. *Curr Biol* 22(12):1047–1056.
3. Mehdizadeh A, Mei R, Klausner JF, Rahmatian N (2010) Interaction forces between soft magnetic particles in uniform and non-uniform magnetic fields. *Acta Mech Sin* 26(6): 921–929.
4. Sugawara T, Kaneko K (2011) Chemophoresis as a driving force for intracellular organization: Theory and application to plasmid partitioning. *Biophys Soc Japan* 7:77–88.

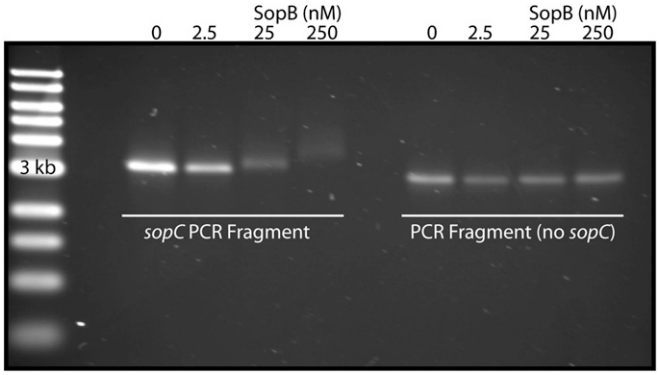

Fig. S1. Site-specific binding of SopB to biotinylated and Alexa 647-labeled *sopC* DNA. The DNA substrate was PCR amplified from a pBR322 plasmid with or without the *sopC* site as indicated. The DNA substrates (2 nM) were incubated with SopB at the concentrations indicated at 30 °C for 30 min. The 20-μL sample was run on a 0.8% agarose gel. Binding to the DNA substrate was dependent upon the presence of *sopC*. The *sopC*-fragment was later conjugated to streptavidin-coated 1-μm magnetic beads (*DNA-Bead Coupling* in *Materials and Methods*).

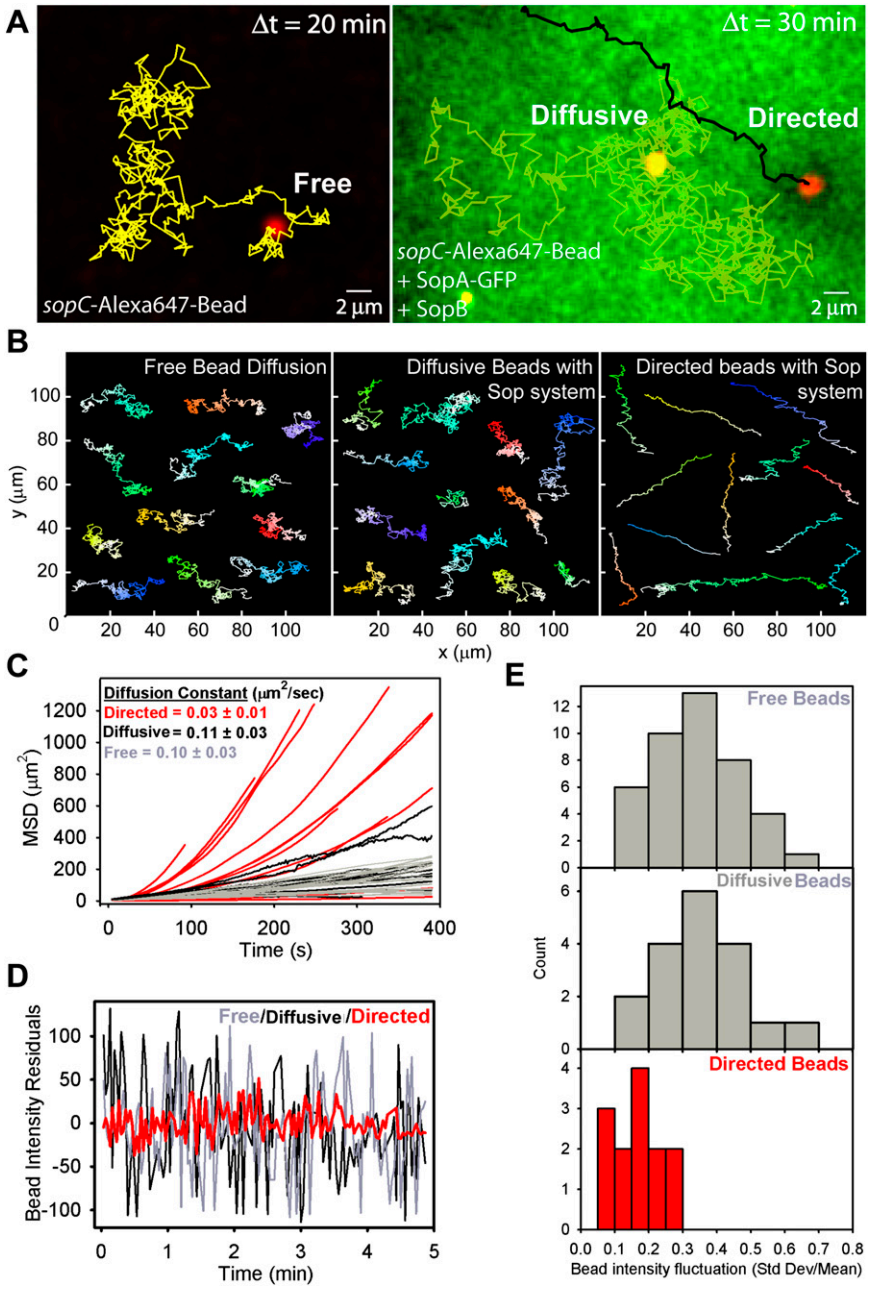

Fig. S2. Directed and diffusive bead dynamics in the presence of the Sop system compared with freely diffusing beads. (*A*) Freeze frames of bead (red) diffusion in the absence (*Left*) or presence (*Right*) of SopA-GFP (green), SopB, and ATP. Free- and diffusive-bead trajectories are represented by yellow lines, and the directed-bead trajectory by a black line. (*B*) Examples of several free (*Left*), diffusive (*Center*), and directed (*Right*) bead trajectories in the absence (*Left*) or presence (*Center* and *Right*) of the Sop system. Light to dark shading of the trajectories shows the start to end temporal progression, respectively. (*C*) Mean square displacement (MSD) of directed (red), diffusive (black), and free (gray) bead populations in *B* plotted against time. The diffusion constant for diffusive- and free-bead populations were calculated from the slope of the linear MSD plots. For directed beads, the diffusion constant was obtained from the slope of the linear term of the quadratic MSD fit (see above). Similar diffusion constants (within the error indicated) were obtained from the SD of the single step size distribution. (*D*) Directed beads maintain an interaction with the carpet. Fluorescence intensity fluctuations of the free, diffusive, and directed beads in *A* were recorded over the course of their trajectories and fit to a linear equation. The residuals were then plotted against time. (*E*) Histogram of bead intensity fluctuations normalized by the mean intensity for the three bead populations.

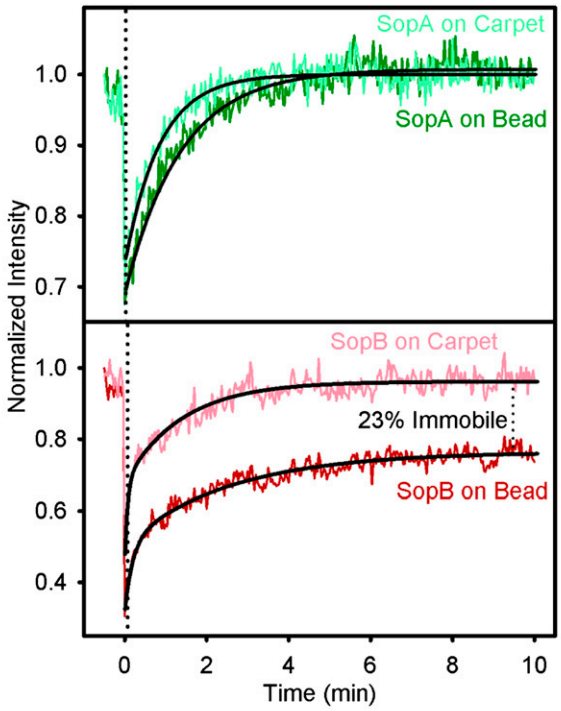

FRAP	t_1 Rate (min^{-1})	t_1 Fraction (%)	t_2 Rate (min^{-1})	t_2 Fraction (%)	Immobile Fraction (%)
SopA on Carpet	1.2 ± 0.1	100 ± 1	--	--	--
SopA on Bead	0.7 ± 0.1	100 ± 3	--	--	--
SopB on Carpet	12.3 ± 2.9	44 ± 3	0.6 ± 0.1	56 ± 1	3 ± 3
SopB on Bead	4.8 ± 0.8	32 ± 2	0.4 ± 0.1	45 ± 1	23 ± 2

Fig. S3. Fluorescence recovery after photobleaching (FRAP) analysis of SopA and SopB exchange on the DNA carpet and bead. FRAP curves were fit to a single exponential for SopA (*Upper*) and a double exponential for SopB (*Lower*). Recovery rates and fractions (as a percentage) are shown in the table. SopA exchange on the bead was slightly slower than that on the DNA carpet. The nonexchanging fraction of SopB on the beads is indicative of *sopC* specific binding. The data are consistent with the proposal that the immobile fraction of SopB is bound specifically to the *sopC* site, and SopB binding to the flanking nonspecific DNA is highly dynamic.

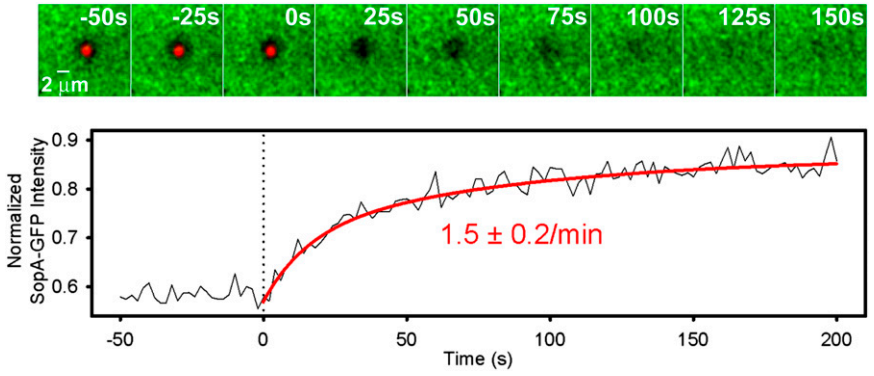

Fig. S4. Magnetic pulling force is required to maintain beads on the carpet. When the magnet was removed ($t = 0$ s), beads fell off the carpet and the SopA depletion zone refilled. SopA rebinding was fit to a single exponential. The SopA depletion zone refilled at a rate of 1.5 ± 0.2 min^{-1}; similar to the SopA exchange rate on the DNA carpet measured by FRAP (Fig. S3). Without the magnet, the system dynamics mirrored what was found previously with plasmid substrates; that is, after initial tethering to the carpet and formation of the SopA depletion zone, the beads detached from the carpet.

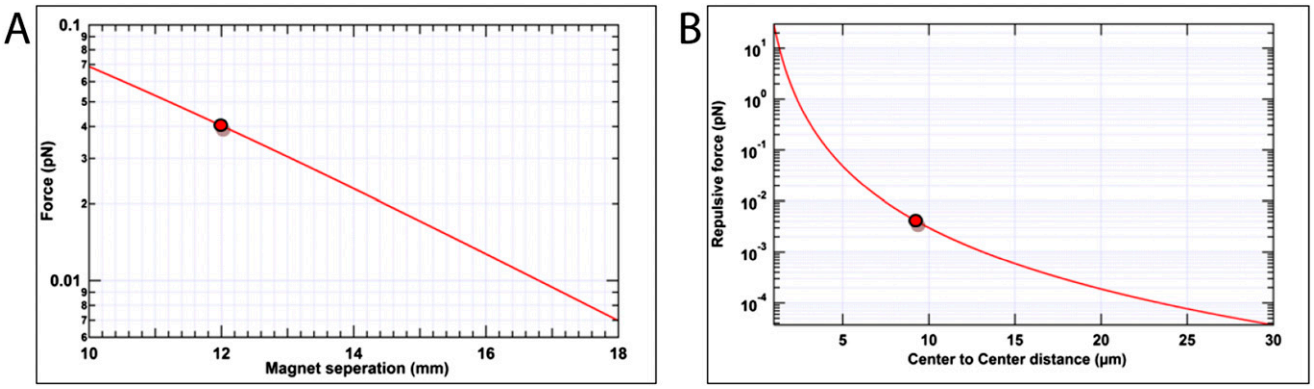

Fig. S5. Vertical and pairwise repulsive forces on magnetic beads. (*A*) The upward force on a Dynal MyOne magnetic bead was plotted as a function of the distance between the end of the magnet and the surface of the flow cell. The red dot indicates the vertical force exerted on a bead (0.04 pN) at the 12-mm magnet separation from the flow cell surface, which was the distance used here. (*B*) Repulsive force on beads as a function of the center-to-center distance. The red dot highlights the repulsive force (0.005 pN) at the distance of closest approach (9 μm) between two beads.

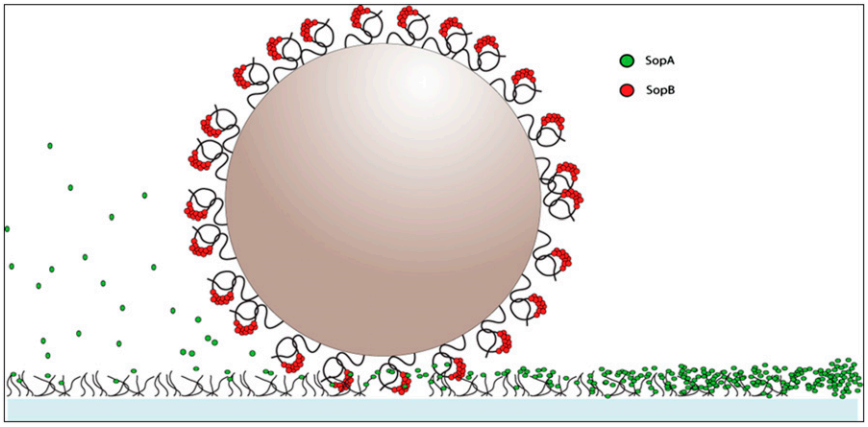

Fig. S6. Schematic of the interaction between the SopB-coated magnetic bead and the SopA gradient on the flow cell surface. SopB (red) binds *sopC* fragments that coat the magnetic bead, and SopA (green) binds to the DNA carpet. SopB stimulates the release of SopA creating a concentration gradient of SopA around the bead. The bead moves directionally as SopB climbs up the concentration gradient toward a greater number of SopA contacts on the DNA carpet. A reversal in bead direction is suppressed by the SopA depletion in the wake of the beads movement.

Table S1. PCR primers used to create *sopC* DNA fragments

Primer name	Sequence, 5′ to 3′	Location on pBR322, bp	Notes
MM1810-BIO	Biotin[3]-CTGCTGAAGCCAGTTACCTTCGG	2,997–3,019	For bead conjugation
MM1810-3K	CCGCGTTTCCAGACTTTACG	1,636–1,619	For unlabeled *sopC*
MM1810-A647	Alexa 647-CCGCGTTTCCAGACTTTACG	1,636–1,619	Alexa 647-labeled *sopC*

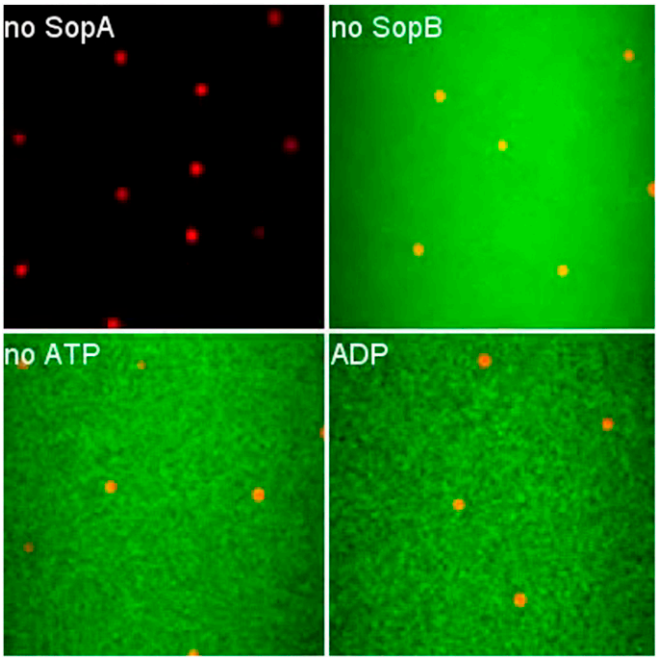

Movie S1. Initial bead tethering requires both Sop proteins and ATP. In the absence of SopA-GFP (*Upper Left*), SopB (*Upper Right*), or ATP (*Lower Left* and *Right*), the beads (red) freely diffused laterally, but are confined within the TIRF illumination volume by the magnet. Movies are 60 times faster than real time. Display areas are 60 × 60 μm.

Movie S1

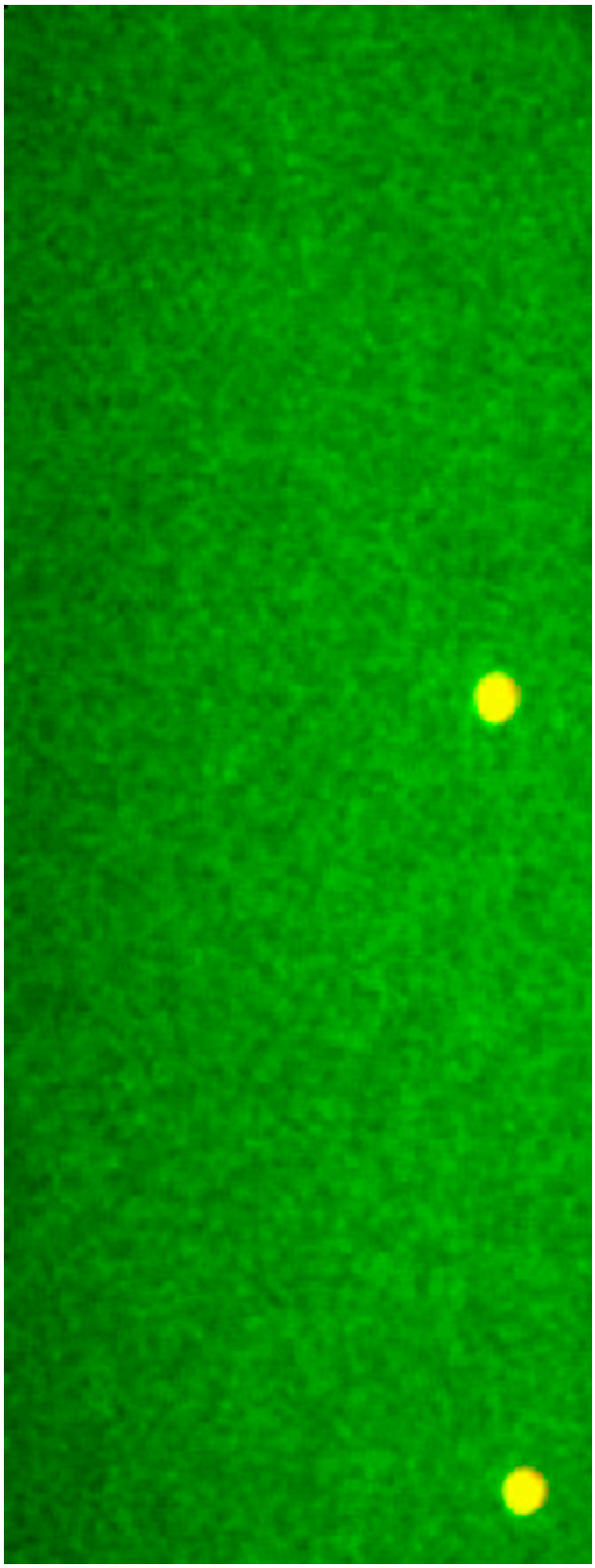

Movie S2. Directed bead movement in the presence of Sop system. With ATP present, SopA-GFP (green) and SopB tether *sopC*-beads (red) to the DNA carpet. As SopA-GFP releases from the bead, it begins traveling laterally on the DNA carpet. Movie is 20 times faster than real time. Display area is 30 × 80 μm.

Movie S2

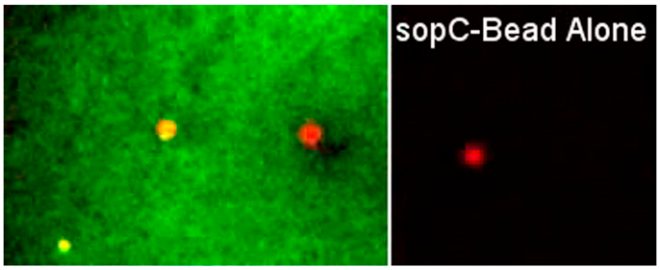

Movie S3. SopA patterning on carpet correlates with directed bead motion. Beads with a SopA depletion zone on the carpet displayed directed motion, whereas those without a depletion zone diffused randomly (*Left*); similar to the free diffusion of beads in the absence of Sop proteins (*Right*). Movies are 30 times faster than real time. Right and left display areas are 40 × 30 μm and 30 × 30 μm, respectively.

Movie S3

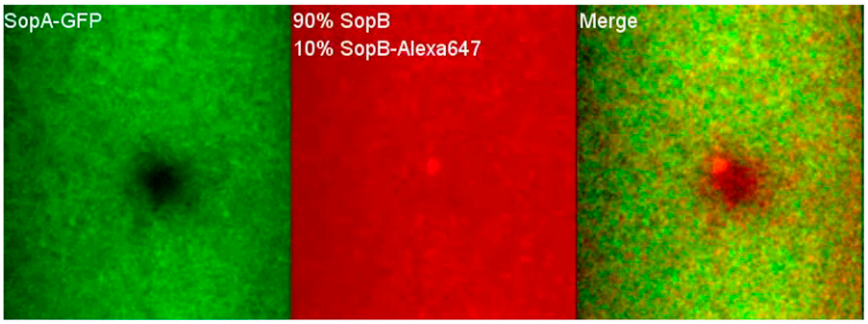

Movie S4. SopB both promotes and follows a SopA gradient on the carpet, resulting in directed bead motion. SopA-GFP depletion (green and merge) is followed by directed motion of the *sopC*-bead bound by SopB-Alexa 647 (red and merge). Movie is 30 times faster than real time. Display areas are 50 × 50 μm.

Movie S4

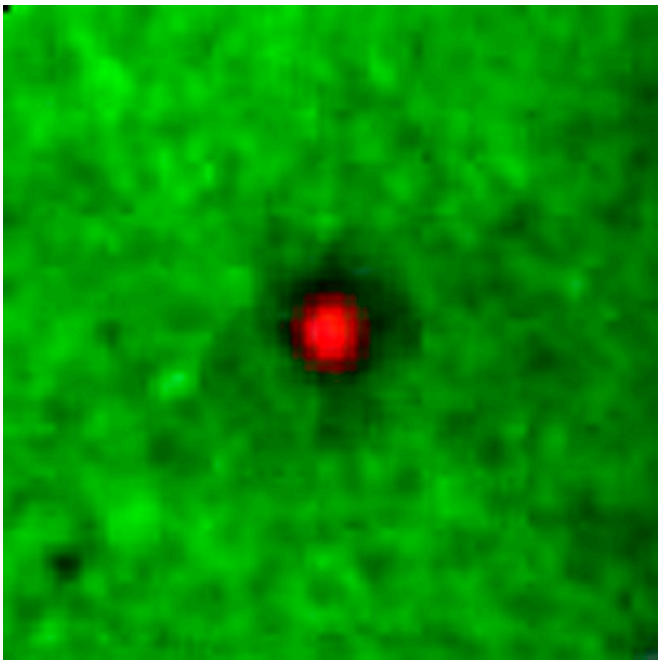

Movie S5. Magnet is required to maintain beads on the DNA carpet. Magnet was raised away from the flow cell surface at $t = 2$ s of the movie. The bead (red) fell into the solution phase of the flow cell and the SopA-GFP (green) depletion zone refilled. Movie is 30 times faster than real time. Display area is 20 × 20 μm.

Movie S5

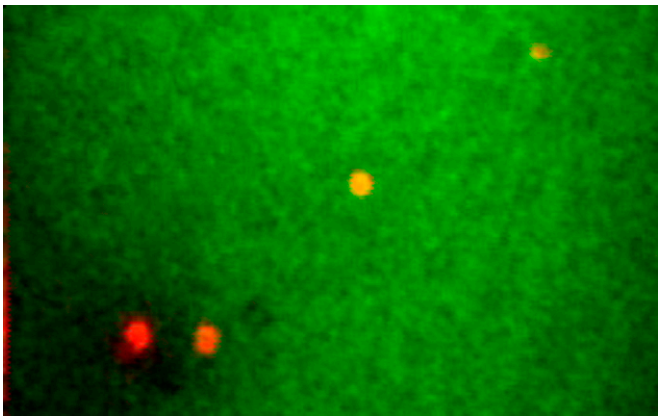

Movie S6. Directed bead movement can bulldoze freely diffusing beads. The vertical magnetic axis induced interbead magnetic repulsion. The repulsive force allowed directed beads to push random beads out of their path. Movie is 60 times faster than real time. Display area is 30 × 50 μm.

Movie S6

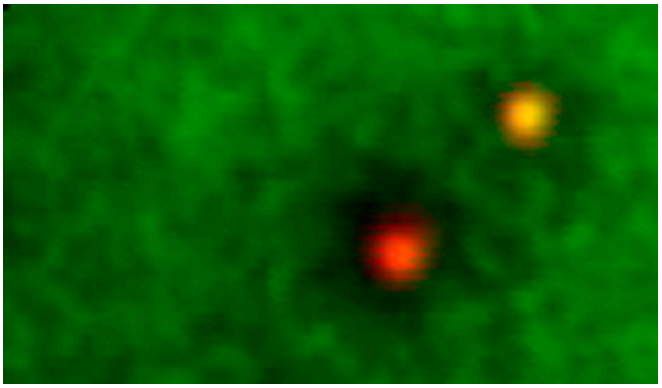

Movie S7. Directed bead motion deflected and stalled by a static bead. Movie is 30 times faster than real time. Display area is 22 × 13 μm.

Movie S7

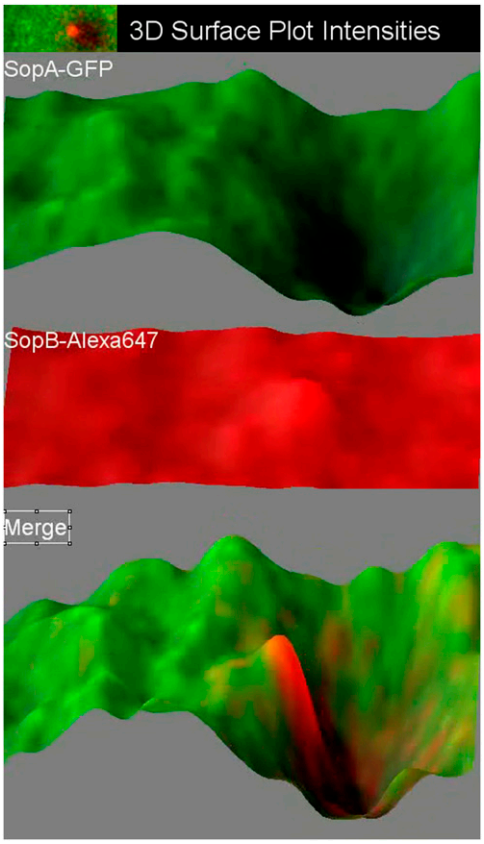

Movie S8. Time-lapse 3D intensity plots of SopA-GFP (green) on the carpet and SopB-Alexa 647 (red) on a directed bead. The lower panel shows the merge. Original movie is displayed at *Upper Left* and is 20 times faster than real time. Display area is 2.5 × 6 μm.

Movie S8

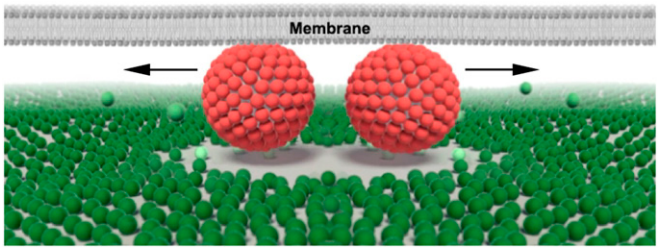

Movie S9. Animation of a diffusion-ratchet model for ParA-mediated transport and partition. Segment 1, system dynamics without surface confinement of the cargo. Segment 2, transport of cargo confined to the nucleoid surface by the inner membrane of a bacterial cell. Segment 3, segregation of surface-confined cargo. Also see Fig. 4 for more details.

Movie S9